SUB-NYQUIST SAMPLING OF OFDM SIGNALS FOR COGNITIVE RADIOS

Tom Zahavy, Oran Shayer, Deborah Cohen, Alex Tolmachev and Yonina C. Eldar

Department of Electrical Engineering, Technion - Israel Institute of Technology

ABSTRACT

We investigate sampling and detection of orthogonal frequency-division multiplexing (OFDM) signals with unknown carriers at sub-Nyquist rates. Efficient acquisition and processing of such broadcast signals is a challenge but constitutes a crucial part of enabling cognitive radios. In order to alleviate both the analog and digital burden when treating wideband signals, we adapt the modulated wideband converter (MWC), a recently proposed sub-Nyquist sampling system, to fit OFDM signals. In particular, after detecting the active bands using the MWC, we use several different equalization methods in order to improve the bit-error rate (BER). We then show how to process the real sub-Nyquist samples in each band in order to recover the complex OFDM signal. A standard digital OFDM receiver is then used to detect the input symbols. To evaluate the performance of our system, we derive an analytical bound on the BER as a function of the received signal to noise ratio. Simulations validate the proposed system.

Index Terms— Compressed sensing, modulated wideband converter, multiband sampling, OFDM, cognitive radios

1. INTRODUCTION

Spectral resources are traditionally allocated to licensed or primary users (PUs) by governmental organizations. Today, most of the spectrum is already owned and new users can hardly find free frequency bands. In light of the ever-increasing demand from new wireless communication users, this issue has become critical over the past few years. Various studies [1, 2, 3] have shown that this over-crowded spectrum is usually significantly underutilized and can be described as the union of a small number of narrowband transmissions spread across a wide spectrum range. This motivates cognitive radios (CR), which allow secondary users to opportunistically use the licensed spectrum when the PU is inactive [4, 5].

One of the crucial tasks in the CR cycle is spectrum sensing [6]. The CR has to constantly monitor the spectrum and detect the PU's activity in order to select unoccupied bands, before and throughout its transmission. At the receiver, the CR samples the signal and performs detection to assert which band can be exploited for opportunistic transmissions. To minimize the interference caused to PUs, the spectrum sensing task performed by a CR must be reliable and fast [7, 8, 9]. On the other hand, in order to increase the chance to find an unoccupied spectral band, the CR has to sense a wide band of spectrum. Nyquist rates of wideband signals are high and can exceed today's best analog-to-digital converters (ADCs) front-end bandwidths. Besides, high sampling rates generate a large number of samples to process, affecting speed and power consumption.

THE AUTHORS 1,2 CONTRIBUTED EQUALLY TO THIS PAPER. THIS WORK IS SUPPORTED BY THE SRC, BY THE ISF UNDER GRANT NO. 170/10 AND BY THE OLLENDORF FOUNDATION.

To overcome the rate bottleneck, several new sampling methods have been proposed [10, 11, 12] that reduce the rate in multiband settings below the Nyquist rate. In [12], the authors present the modulated wideband converter (MWC), a sub-Nyquist system, that purposely aliases the signal and samples it at a low rate. Recovery techniques that exploit compressed sensing methods are then utilized after sampling to identify the signal support. The paper considers general modulation types and focuses on support recovery.

In this paper, we consider orthogonal frequency-division multiplexing (OFDM) modulation, which is the most common broadcasting method today. We follow the basic configuration of the 4G LTE E-UTRA standard. We aim to show, as far as we know for the first time, sampling of an OFDM signal and detection of its encoded symbols from sub-Nyquist time domain samples without knowing its carriers and with no prior knowledge of the signal except for sparsity in frequency. In [13, 14] the authors consider a sparse OFDM signal with known sub-carriers. The signal is recontructed from its sub-Nyquist samples, by exploiting this *a priori* knowledge of the potentially active sub-carriers. The works of [15, 16] offer CS techniques for spectrum sensing however they do not detect the digital symbols themselves but rather the power spectrum of the OFDM signal.

We present the MWC-OFDM system, which samples a wideband signal composed of several OFDM transmissions with unknown carriers at a sub-Nyquist rate. Our approach is completely compatible with standard digital OFDM detectors so that after our poposed processing, a standard OFDM receiver can be used on the sub-Nyquist samples. We use the MWC [12] for the sampling stage and support recovery. The encoded digital data is then recovered through blind signal reconstruction. The MWC-OFDM architecture consists of (1) OFDM transmitter (2) MWC - mixing, sampling (3) post-processing tailored to OFDM signals (4) digital OFDM receiver. Our main contribution is the inscription of sub-Nyquist sampling performed by the MWC in a real communication scenario. In order to reconstruct the input signal from its sub-Nyquist samples, we investigate several equalization techniques. We then derive a reconstruction method for recovering the original complex signal from real samples. This processing is back compatible with a regular digital OFDM receiver. The performance of the MWC-OFDM receiver is evaluated in terms of bit error rate (BER) as a function of the received signal to noise ratio (SNR). Last, we derive an analytical bound on the performance of symbol recovery from sub-Nyquist samples in noisy settings. Simulations show that we can obtain degradation of less than 0.5dB from this theoretical bound.

2. SYSTEM MODEL AND PROBLEM STATEMENT

OFDM is a popular modulation scheme used in applications such as digital television and audio broadcasting, wireless networks, and 4G mobile communications. It extends the concept of single carrier

978-1-4799-2893-4/14/$31.00 ©2014 IEEE

modulation by using multiple orthogonal subcarriers within the same single channel. Here we consider a multiband model, as described in [12], in combination with OFDM.

We consider N OFDM transmissions spread arbitrarily within some large bandwidth, which we denote by BW. We also define f_{max} as the maximal frequency that data could be transmited on and accordingly we define f_{min} as the minimal frequency that data could be transmitted on, so that $BW = f_{max} - f_{min}$. Note that BW is the possible occupied bandwidth on each side of the frequency axis, positive and negative. The carrier frequencies are assumed to be unknown. Each transmission is an independent OFDM signal with bandwidth B.

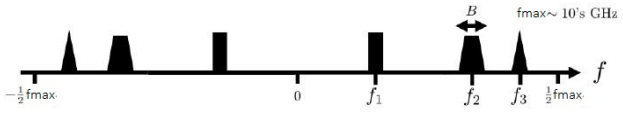

Fig. 1. Typical spectrum support of a multiband signal composed of three OFDM transmissions.

When transmitting an OFDM signal, the first step is to encode the information bits into symbols using a modulator. We use a 4-QAM modulator and denote the series of symbols by $X_k[m]$. The inverse fast Fourier transform (IFFT) is then applied to N_f symbols to yield

$$x_k[n] = \frac{1}{\sqrt{N_f}} \sum_{p=0}^{N_f-1} X_k[p] e^{\frac{j2\pi np}{N_f}}. \quad (1)$$

Next, the digital signal $x_k[n]$ passes through a digital to analog converter (DAC) creating a continuous time signal

$$x_k(t) = \sum_{n=-\infty}^{\infty} x_k[n] g(t - nT_s), \quad (2)$$

where $T_s = \frac{1}{f_s}$ is the symbol rate and $g(t)$ is a lowpass filter shape, which will be specified later on. The signal is then I-Q modulated, in order to transmit a real signal at high frequencies. The transmitted signal is then given by

$$s_k(t) = \mathbb{R}\{x_k(t)\} \cos(2\pi f_k t) - \mathbb{I}\{x_k(t)\} \sin(2\pi f_k t), \quad (3)$$

where $s_k(t)$ stands for the kth OFDM transmission with carrier f_k. The final signal is composed of N OFDM transmissions and is given by $s(t) = \sum_{k=0}^{N-1} s_k(t)$. Standard OFDM receivers consist of analog I-Q demodulation block and a digital processing unit as shown in Fig. 2. In Section 3, we describe our modified receiver that blindly reconstructs the signal from sub-Nyquist samples before performing QAM symbol detection.

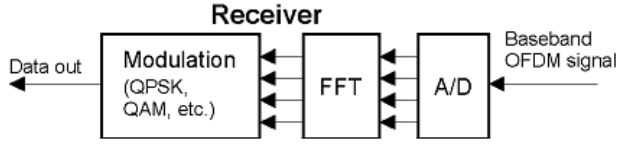

Fig. 2. Ideal OFDM digital receiver: ADC, FFT block and a QAM demodulator [17].

Since the carriers are unknown, the Nyquist rate of the signal is given by $f_{nyq} = 2BW$, and the standard approach is to sample at this rate, which may exceed the specifications of the best analog-to-digital converters (ADCs) by orders of magnitude and will result in a tremendous amount of samples to be processed. Thus, sampling at f_{nyq} is not an efficient option. Our goal is to sample the transmitted signal at a rate lower than f_{nyq}, but still allow data decoding with low BER. In [11], the authors show that the minimal rate allowing for perfect recovery of a signal from the multiband model in a noiseless environment is twice the Landau rate [18], namely $4NB$.

In the simulations, we consider 4G LTE signals, in which channel carriers can be in the range of $f_{min} = 0.7_{GHZ}$ to $f_{max} = 2.1_{GHZ}$ ($BW = 1.4_{GHZ}$). The FFT size is 2048 and a typical channel bandwidth is B=20MHz.

3. THE MWC FOR OFDM SIGNALS

The MWC is a sub-Nyquist sampling system designed for sampling sparse wideband analog signals. It consists of two stages: sampling and reconstruction. In this section, we introduce the mechanism and principles of MWC sampling. Then, we detail the additional OFDM processing that is needed after the MWC and prior to the standard receiver chain, to perform I-Q demodulation.

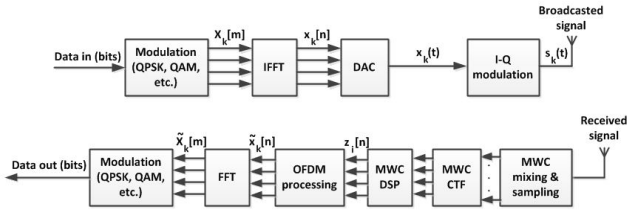

Fig. 3. High-level architecture of the MWC-OFDM.

Figure 3 shows the MWC-OFDM architecture. The system is composed of (a) OFDM transmitter introduced in Section 2. (b) MWC mixing and sampling block which we describe in Section 3.1. (c) Continuous to finite (CTF) block as proposed in [12] for support detection. (d) MWC DSP block for signal reconstruction which we describe in Section 3.2. (e) OFDM processing block described in Section 3.3. (f) digital OFDM receiver.

3.1. MWC Mixing and Sampling

The MWC [12] is composed of m parallel channels. In each channel, an analog mixing front-end, where $x(t)$ is multiplied by a mixing function $p_i(t)$, aliases the spectrum, so that each band appears in baseband. The mixing functions $p_i(t)$ are required to be periodic. We denote by T_p their period and we only require $f_p = \frac{1}{T_p} \geq B$. The function $p_i(t)$ has a Fourier expansion

$$p_i(t) = \sum_{l=-\infty}^{\infty} c_{il} e^{j\frac{2\pi}{T_p} lt}. \quad (4)$$

In each channel, the signal goes through a lowpass filter with cut-off frequency $\frac{f_s}{2}$ and is sampled at rate $\frac{1}{T_s} = f_s \geq f_p$. The samples of the i-th channel are denoted by $y_i[n]$. For simplicity, we choose $f_s = f_p$. In [19] the authors investigate the effect of non-ideal filters on the MWC and develop the perfect reconstruction

(PR) condition. We use a raised cosine lowpass filter that satisfies this condition.

The overall sampling rate is $m \cdot f_s$ where $m \leq L$. We also define $L_0 = \left\lceil \frac{2 \cdot f_{masx} + fs}{2 f_p} \right\rceil - 1$ where $L = 2L_0 + 1$ as calculated in [12] and $L_{LTE} = 211$. The relation between the known DTFTs of the samples $y_i[n]$ and the unknown $X(f)$ can be written as

$$\mathbf{y}(f) = \mathbf{A}\mathbf{z}(f), \qquad f \in \mathcal{F}_s, \tag{5}$$

where $\mathbf{y}(f)$ is a vector of length m where the ith element $y_i(f)$ is the DTFT of $y_i[n]$ and $\mathcal{F}_s = [-\frac{f_s}{2}, \frac{f_s}{2}]$. The unknown vector $\mathbf{z}(f)$ is of length $L = 2L_0 + 1$ with

$$z_i(f) = X(f + (i - L_0 - 1)f_{p)}), \quad 1 \leq i \leq L. \tag{6}$$

The $m \times L$ matrix $\mathbf{A}$ contains the coefficients c_{il} , such that $\mathbf{A}_{il} = c_{i,-l} = c_{il}^*$ with $M \geq L$. Reconstructing $\mathbf{z}(f)$ for all $f \in \mathcal{F}_s$ is equivalent to recovering $X(f)$ for all $f \in \left[-\frac{f_{max}}{2}, \frac{f_{max}}{2}\right]$. We note that $m < L$ for the overall sampling rate to be below the Nyquist rate, leading to an underdetermined system.

3.2. MWC Reconstruction

The reconstruction part consists of two stages carried out in the time domain. First, we perform spectral support recovery, which relies on recent ideas developed in the context of analog compressed sensing [20]. It is implemented by a series of digital computations, which are grouped under the Continuous-to-Finite (CTF) block that determines the support S [12]. The basic CS model we try to solve is given by

$$\mathbf{y}[n] = \mathbf{A}(\mathbf{z}[n] + \mathbf{e}[n]), \tag{7}$$

where $\mathbf{z}[n], \mathbf{y}[n]$ are the IDTFT transforms of $\mathbf{z}(f), \mathbf{y}(f)$ and $\mathbf{e}[n]$ is additive noise with variance σ^2. The unknown vector $\mathbf{z}[n]$ can be reconstructed as follows [12]

$$\mathbf{z}_S[n] z_i[n] = \mathbf{A}_S^{\dagger} \mathbf{y}[n], = 0, \; i \notin S. \tag{8}$$

Here, the submatrix $\mathbf{A}_S$ is comprised of the columns of $\mathbf{A}$ indexed by S, the vector $\mathbf{z}_S[n]$ is comprised of the elements of $\mathbf{z}[n]$ indexed by S and the notation $(\cdot)^{\dagger}$ denotes the Moore-Penrose pseudo inverse. This reconstruction method, or linear equalization, is formally known as zero-forcing (ZF).

There are several linear equalization methods that may produce better performance depending on the SNR. In this paper we present results of simulations with several reconstructions methods we applied to the MWC. In particular, we examine matched filtering (MF), corresponding to

$$\mathbf{z}_s[n] = \mathbf{A}_s^* \mathbf{y}[n]. \tag{9}$$

We also examine Wiener filtering, taking into consideration that our noise is not white, but is colored with covariance $\mathbf{C} = \sigma^2 \mathbf{A}\mathbf{A}^*$. This leads to the following reconstruction formula:

$$\mathbf{z}_s[n] = (\mathbf{A}_s^*(\mathbf{A}\mathbf{A}^*)^{-1}\mathbf{A}_s + \sigma^2 \mathbf{I})^{-1} \mathbf{A}_s^*(\mathbf{A}\mathbf{A}^*)^{-1} \mathbf{y}[n]. \tag{10}$$

Another approach we examined is using pre-whitening techniques. Let $\mathbf{B} = (\mathbf{A}\mathbf{A}^t)^{-1/2}$ and define $\tilde{\mathbf{y}} = \mathbf{B}\mathbf{y}$. This leads us to the following ZF and MF reconstruction, respectively:

$$\mathbf{z}_s[n] = (\mathbf{A}_s^*(\mathbf{A}\mathbf{A}^*)^{-1}\mathbf{A}_s)^{-1} \mathbf{A}_s^*(\mathbf{A}\mathbf{A}^*)^{-1} \mathbf{y}[n], \tag{11}$$

$$\mathbf{z}_s[n] = \mathbf{A}_s^*(\mathbf{A}\mathbf{A}^*)^{-1} \mathbf{y}[n]. \tag{12}$$

Additional explanations and details can be found in [21].

To ensure good performance in the presence of noise, as explained in [22], the matrix $\mathbf{A}$ should be chosen as close to unitary as possible. While a variety of sequences have been suggested for the MWC [23], we focused on the Legendre sequence from [24] which result in a matrix very close to unitary. The matrix $\mathbf{A}$ is a $m \times L$ binary pattern, where the expression for the basic sequence is given by

$$C_0 = 1, \;\; C_i = \begin{cases} +1, & \text{if } i \text{ is a square} \\ -1, & \text{if } i \text{ is a non-square} \end{cases} \quad i > 1. \tag{13}$$

The matrix $\mathbf{A}$ is then constructed by randomly shifting this sequence as described in [24].

Once the lowrate sequences of the spectrum slices $z_i[n]$ are recovered at the DSP unit, they pass to the next unit, namely OFDM processing.

3.3. OFDM processing

As explained in (2), the digital receiver expects to receive samples of an I-Q demodulated signal, which can be expressed as

$$x_k[n] = \{[y(t) \cdot (\cos(2\pi f_k t) - j \sin(2\pi f_k t))] * h(t)\}_{t = nT_s}. \tag{14}$$

Here $y(t)$ is the received analog signal, and $h(t)$ is the impulse response of the antialiasing lowpass filter, used before sampling. We have seen that the MWC outputs every spectrum slice from the received signal as lowrate sequences around baseband, denoted by $z_i[n]$. Our goal now is to process these sequences in order to provide the required samples to the digital receiver.

We focus on a single transmitted signal in order to analyze the processing needed. The OFDM signal before broadcast is $x_k(t) = r_k(t) + j \cdot i_k(t)$, where $r_k(t)$ and $i_k(t)$ stands for the real and imaginary parts of the signal, respectively. The transmitted signal after I-Q modulation is given by (3) and its Fourier transform is

$$S_k(f) = \frac{1}{2}\left[R_k(f - f_k) + R_k(f + f_k)\right] + \\ + \frac{j}{2}\left[I_k(f - f_k) - I_k(f + f_k)\right]. \tag{15}$$

Consider the positive and negative frequency parts of $S_k(f)$

$$S_{k\pm}(f) = \frac{1}{2}\left[R(f \mp f_c) \pm j \cdot I(f \mp f_c)\right]. \tag{16}$$

After passing the transmitted signal $s_k(t)$ through the MWC, each low-rate sequence $z_i[n]$ represents either a positive or negative spectrum slice around baseband. We denote by $z_{i+}(f)$ a positive spectrum slice and by $z_{i-}(f)$ its corresponding negative slice. The spectrum slices can be written explicitly as

$$z_{i\pm}(f) = \frac{1}{2}\left[R(f) \pm j \cdot I(f)\right]. \tag{17}$$

Thus, in order to recover the real (imaginary) part of the original OFDM transmission $x_k[n]$ before I-Q modulation, we add (substract) the low-rate sequence representing the negative spectrum slice and its corresponding positive spectrum slice:

$$x_k[n] = [z_{k+}[n] + z_{k-}[n]] + j\left[z_{k+}[n] - z_{k-}[n]\right]. \tag{18}$$

Without noise, these recovered samples are exactly the samples the digital receiver expects. We note that by adding the positive and negative spectrum slices we effectively improve the SNR of the real and imaginary parts by a factor of 2, thus allowing the same performance as in sampling I and Q seperately. This processing stage allows us to continue with $x_k(t)$ as inputs into the digital receiver.

4. BER MEASUREMENT

In this section we demonstrate the proposed architecture performence by experimental results. We also explain why sampling below the Nyquist frequency leads to noise folding.

4.1. Effective noise

Consider a scenario where a single OFDM transmission with unknown carrier from the LTE model is to be sampled. One approach is to sample the entire LTE spectrum of $BW = (0.7_{GHZ} - 2.1_{GHZ})$ at the Nyquist rate. Using demodulation of the entire spectrum to baseband and then sampling will result in a total sampling rate of $f_{\text{Nyq}} = 1.4 \cdot 2 = 2.8_{GHZ}$ where the factor 2 comes from the double sampling for I-Q demodulation. Any method for sampling of the entire BW at a lower rate will result in aliasing of both signal and noise. As explained in [22], the gain in noise due to this aliasing effect is given by $NG = \frac{BW \cdot 2}{f_{total}}$. In order to lower the noise gain (NG) , we use a bandpass filter and filter the signal to the effective spectrum. We denote by $L_{eff} = \frac{2 \cdot BW}{f_s}$ the number of spectrum slices containing energy. Since the total sampling rate of the MWC system is $f_{total} = mf_s$ we define the ideal NG as

$$NG_{ideal} = \frac{L_{eff}}{m}. \tag{19}$$

Note that (19) introduces a tradeoff between the sampling rate and the NG which we are able to measure. As explained in [25], OFDM system performance is measured in terms of BER. Knowing the modulation method, the system is characterized by a unique BER curve as a function of the noise (measured by $\frac{E_b}{N_0}\text{dB}$). Since the noise in the system is amplified we expect to measure a BER curve shifted by $10\log_{10}(NG)$. The lowest shift that can be achieved is by NG_{ideal}, leading to a minimal BER of BER_{ideal}. Thus, our performance must be limited by BER_{ideal}. We now show that our system allows us to get very close to this limit.

4.2. Experimental validation

We now simulate the proposed MWC-OFDM system and examine its performance with a broadcasted 4G LTE signal. When choosing the system parameters, we aimed for simulating a practical system. Thus, we chose a non-ideal lowpass filter as described in Section 3.1 and selected the MWC sampling rate as $f_s = f_p = B$, which is the minimal possible rate. The signal is broadcasted with a carrier at 1_{GHz}, which is unknown to the system and corrupted by additive white Gaussian noise. Our results are averaged over 10 realizations of the Legendre sequences. We measure BER in a noisy environment under different reconstruction methods and compare the results with the theoretical curve, BER_{Ideal}.

Fig. 4 presents BER mesurments as a function of SNR for a system with 71 hardware channels. The best reconstruction scheme is the MF which is also the easiest to implement since it does not require any matrix inversion. This is not surprising since the Legendre sequences result in a matrix AA^* that is close to I . The total sampling rate is given by $f_{total} = 71 \cdot 20_{MHZ} = 1.42_{GHz} = \frac{f_{nyq}}{2}$.

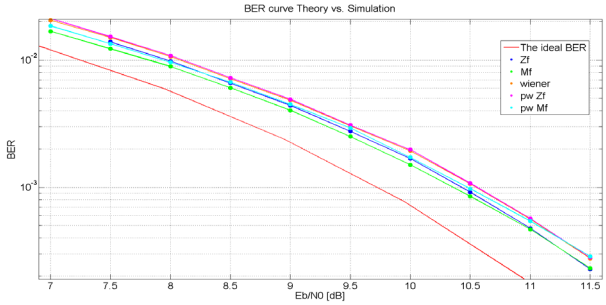

Fig. 4. BER as a function of SNR for 71 channels.

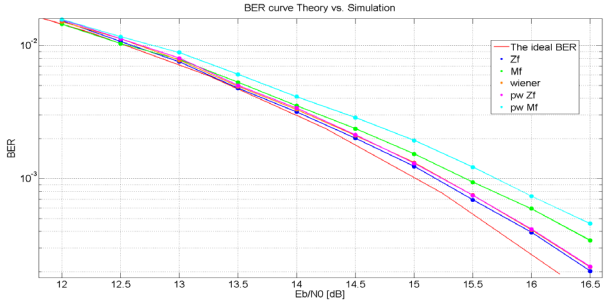

Fig. 5. BER as a function of SNR for 21 channels.

Fig. 5 presents the same scenario but for 21 hardware channels. The total sampling rate is given by $f_{total} = 21 \cdot 20_{MHZ} = 0.42_{GHZ} = \frac{f_{nyq}}{6}$ and the best scheme in this case is ZF. Both figures show a 0.5_{dB} shift in the SNR value from the theory curve. This may be explained by the non-ideality of the sytem and implies that the number of hardware channels does not influence the shift in SNR from the theory curve.

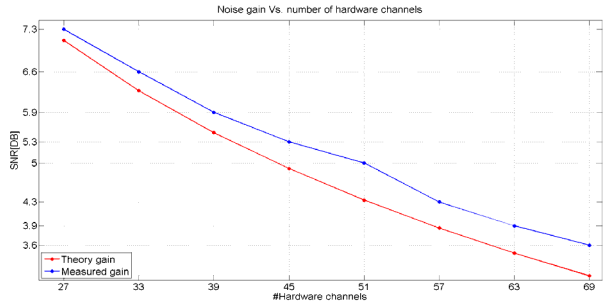

Fig. 6. Trade off between the sampling rate and SNR. The theoretical gain is given by $10\log_{10}(\frac{L_{eff}}{m})$ (19).

In Fig. 6 we compare the performance of the MWC system as a function of the number of hardware channels and measure BER. Measurements were performed with $SNR = 8_{\text{dB}}$ and $21 \leq m \leq 69$. Assuming that the noise is white, we may deduce the effective SNR from the measured BER . This reasoning shows that there is around 0.5dB shift for a given number of channels from the theoretical curve which is consistent with the previous figures, so our system is close to optimal.

5. REFERENCES

[1] FCC, "Spectrum policy task force report: Federal communications commission, tech. rep. 02-135. [online]," *http://www.gov/edocs_public/attachmatch/DOC228542A1.pdf*, Nov. 2002.

[2] M. McHenry, "NSF spectrum occupancy measurements project summary. shared spectrum co., tech. rep. [online]," *http://www.sharedspectrum.com*, Aug. 2005.

[3] R. I. C. Chiang, G. B. Rowe, and K. W. Sowerby, "A quantitative analysis of spectral occupancy measurements for cognitive radio," *Proc. of IEEE Vehicular Technology Conference*, pp. 3016–3020, Apr. 2007.

[4] J. Mitola, "Software radios: Survey, critical evaluation and future directions," *IEEE Aerosp. Electron. Syst. Mag*, vol. 8, pp. 25–36, Apr. 1993.

[5] S. Haykin, "Cognitive radio: Brain-empowered wireless communications," *IEEE J. Select. Areas Commun.*, vol. 23, pp. 201–220, Feb. 2005.

[6] A. Ghasemi and E. S. Sousa, "Spectrum sensing in cognitive radio networks: requirements, challenges and design tradeoffs," *IEEE Communications Magazine*, vol. 46, pp. 32–39, Apr. 2008.

[7] N. Hoven A. Sahai and R. Tandra, "Some fundamental limits on cognitive radio," *Proc. 42nd Annu. Allerton Conf. Communication, Control, and Computing*, pp. 1662–1671, Oct. 2004.

[8] E. G. Larsson and M. Skoglund, "Cognitive radio in a frequency-planned environment: Some basic limits," *IEEE Trans. Wireless Commun.*, vol. 7, pp. 4800–4806, Dec. 2008.

[9] Moshe Mishali and Yonina C Eldar, "Wideband spectrum sensing at sub-nyquist rates [applications corner]," *Signal Processing Magazine, IEEE*, vol. 28, no. 4, pp. 102–135, 2011.

[10] M. Mishali and Y. C. Eldar, "Sub-Nyquist sampling: Bridging theory and practice," *IEEE Signal Proc. Magazine*, vol. 28, no. 6, pp. 98–124, Nov. 2011.

[11] M. Mishali and Y. C. Eldar, "Blind multi-band signal reconstruction: Compressed sensing for analog signals," *IEEE Trans. on Signal Processing*, vol. 57, no. 3, pp. 993–1009, Mar. 2009.

[12] M. Mishali and Y. C. Eldar, "From theory to practice: Sub-Nyquist sampling of sparse wideband analog signals," *Selected Topics in Signal Processing, IEEE Journal of*, vol. 4, no. 2, pp. 375–391, 2010.

[13] S. Hoyos Z. Yu and B. Sadler, "Mixed-signal parallel compressed sensing and reception for cognitive radio," in *Acoustics, Speech and Signal Processing, 2008. ICASSP 2008. IEEE International Conference on*. IEEE, 2008, pp. 3861–3864.

[14] A. Griffin T. Agrawal, V. Lakkundi and P. Tsakalides, "Compressed sensing for OFDM UWB systems," in *Radio and Wireless Symposium (RWS), 2011 IEEE*. IEEE, 2011, pp. 190–193.

[15] D. D. Arianandа and G. Leus, "Wideband power spectrum sensing using sub-Nyquist sampling," in *Signal Processing Advances in Wireless Communications (SPAWC), 2011 IEEE 12th International Workshop on*. IEEE, 2011, pp. 101–105.

[16] A. Pandharipande G. Leust Y. L. Polo, Y. Wang, "Compressive wide-band spectrum sensing," in *Acoustics, Speech and Signal Processing, 2009. ICASSP 2009. IEEE International Conference on*. IEEE, 2009, pp. 2337–2340.

[17] E. Lawrey, *The suitability of OFDM as a modulation technique for wireless telecommunications, with a CDMA comparison.*, Ph.D. thesis, James Cook University, 2001.

[18] H. Landau, "Necessary density conditions for sampling and interpolation of certain entire functions," *Acta Math*, vol. 117, pp. 37–52, 1967.

[19] Y. C. Eldar Y. Chen, M. Mishali and A. O. Hero, "Modulated wideband converter with non-ideal lowpass filters," in *Acoustics Speech and Signal Processing (ICASSP), 2010 IEEE International Conference on*. IEEE, 2010, pp. 3630–3633.

[20] Yonina C Eldar, "Compressed sensing of analog signals in shift-invariant spaces," *Signal Processing, IEEE Transactions on*, vol. 57, no. 8, pp. 2986–2997, 2009.

[21] B. Sklar, *Digital communications: fundamentals and applications*, Prentice-Hall, Inc., Upper Saddle River, NJ, USA, 1988.

[22] E. Ariass-Castro and Y. C. Eldar, "Noise folding in compressed sensing," *Signal Processing Letters, IEEE*, vol. 18, no. 8, pp. 478–481, 2011.

[23] M. Mishali and Y. C. Eldar, "Expected RIP: Conditioning of the modulated wideband converter," in *Information Theory Workshop, 2009. ITW 2009. IEEE*. IEEE, 2009, pp. 343–347.

[24] H. Wang L. Gan, "Deterministic binary sequences for modulated wideband converter," *Proceedings of the 10th International Conference on Sampling Theory and Applications*, 2013.

[25] E. Lee J. Barry and D. Messerschmitt, *Digital communications*, Springer, 2004.